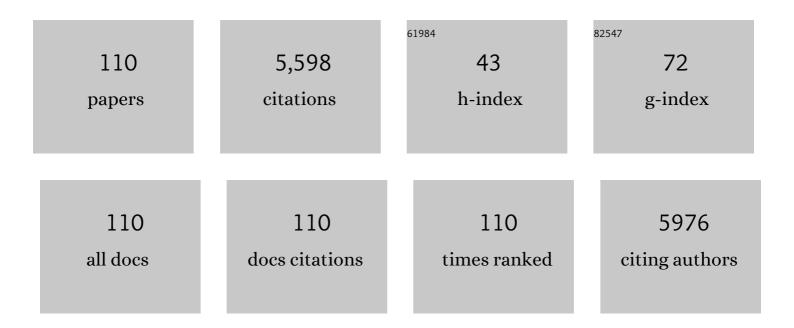


List of Publications by Year in descending order

Source: https://exaly.com/author-pdf/1119497/publications.pdf Version: 2024-02-01



#	Article	IF	CITATIONS
1	Decolorization of Azo Dyes in Bioelectrochemical Systems. Environmental Science & Technology, 2009, 43, 5137-5143.	10.0	299
2	Insight into electro-Fenton and photo-Fenton for the degradation of antibiotics: Mechanism study and research gaps. Chemical Engineering Journal, 2018, 347, 379-397.	12.7	287
3	Degradation Chemistry and Stabilization of Exfoliated Few-Layer Black Phosphorus in Water. Journal of the American Chemical Society, 2018, 140, 7561-7567.	13.7	273
4	Defective titanium dioxide single crystals exposed by high-energy {001} facets for efficient oxygen reduction. Nature Communications, 2015, 6, 8696.	12.8	263
5	Nitrobenzene Removal in Bioelectrochemical Systems. Environmental Science & Technology, 2009, 43, 8690-8695.	10.0	191
6	Reductive degradation of nitrobenzene in aqueous solution by zero-valent iron. Chemosphere, 2004, 54, 789-794.	8.2	175
7	Effects of Molecular Structure on Organic Contaminants' Degradation Efficiency and Dominant ROS in the Advanced Oxidation Process with Multiple ROS. Environmental Science & Technology, 2022, 56, 8784-8795.	10.0	161
8	Kinetic modeling of batch hydrogen production process by mixed anaerobic cultures. Bioresource Technology, 2006, 97, 1302-1307.	9.6	150
9	Enhancing Extracellular Electron Transfer of <i>Shewanella oneidensis</i> MR-1 through Coupling Improved Flavin Synthesis and Metal-Reducing Conduit for Pollutant Degradation. Environmental Science & Technology, 2017, 51, 5082-5089.	10.0	141
10	A kinetic approach to anaerobic hydrogen-producing process. Water Research, 2007, 41, 1152-1160.	11.3	137
11	Biological hydrogen production in a UASB reactor with granules. I: Physicochemical characteristics of hydrogen-producing granules. Biotechnology and Bioengineering, 2006, 94, 980-987.	3.3	118
12	Electron acceptors for energy generation in microbial fuel cells fed with wastewaters: A mini-review. Chemosphere, 2015, 140, 12-17.	8.2	116
13	Impact of zero-valent iron nanoparticles on the activity of anaerobic granular sludge: From macroscopic to microcosmic investigation. Water Research, 2017, 127, 32-40.	11.3	110
14	Efficient nitro reduction and dechlorination of 2,4-dinitrochlorobenzene through the integration of bioelectrochemical system into upflow anaerobic sludge blanket: A comprehensive study. Water Research, 2016, 88, 257-265.	11.3	102
15	Substantial enhancement of anaerobic pyridine bio-mineralization by electrical stimulation. Water Research, 2018, 130, 291-299.	11.3	101
16	Remediation of Petroleum-Contaminated Soil and Simultaneous Recovery of Oil by Fast Pyrolysis. Environmental Science & Technology, 2018, 52, 5330-5338.	10.0	87
17	Decoupling of DAMO archaea from DAMO bacteria in a methane-driven microbial fuel cell. Water Research, 2017, 110, 112-119.	11.3	86
18	Coupling of a bioelectrochemical system for p-nitrophenol removal in an upflow anaerobic sludge blanket reactor. Water Research, 2014, 67, 11-18.	11.3	85

#	Article	IF	CITATIONS
19	Microbial electrochemistry for bioremediation. Environmental Science and Ecotechnology, 2020, 1, 100013.	13.5	83
20	The role of pH in the fermentative H2 production from an acidogenic granule-based reactor. Chemosphere, 2006, 64, 350-358.	8.2	76
21	Stimulation of oxygen to bioanode for energy recovery from recalcitrant organic matter aniline inÂmicrobial fuel cells (MFCs). Water Research, 2015, 81, 72-83.	11.3	76
22	Interactions between nanoscale zero valent iron and extracellular polymeric substances of anaerobic sludge. Water Research, 2020, 178, 115817.	11.3	74
23	Carbonate-activated hydrogen peroxide oxidation process for azo dye decolorization: Process, kinetics, and mechanisms. Chemosphere, 2018, 192, 372-378.	8.2	72
24	Efficient activation of PAA by FeS for fast removal of pharmaceuticals: The dual role of sulfur species in regulating the reactive oxidized species. Water Research, 2022, 217, 118402.	11.3	66
25	Coupling of iron shavings into the anaerobic system for enhanced 2,4-dinitroanisole reduction in wastewater. Water Research, 2016, 101, 457-466.	11.3	63
26	Rheological and fractal characteristics of granular sludge in an upflow anaerobic reactor. Water Research, 2006, 40, 3596-3602.	11.3	61
27	A modeling approach to describe ZVI-based anaerobic system. Water Research, 2013, 47, 6007-6013.	11.3	60
28	Enhancement of azo dye decolourization in a MFC–MEC coupled system. Bioresource Technology, 2016, 202, 93-100.	9.6	60
29	Facilitated bio-mineralization of N,N-dimethylformamide in anoxic denitrification system: Long-term performance and biological mechanism. Water Research, 2020, 186, 116306.	11.3	60
30	Substantially enhanced anaerobic reduction of nitrobenzene by biochar stabilized sulfide-modified nanoscale zero-valent iron: Process and mechanisms. Environment International, 2019, 131, 105020.	10.0	59
31	Rapid Release of Arsenite from Roxarsone Bioreduction by Exoelectrogenic Bacteria. Environmental Science and Technology Letters, 2017, 4, 350-355.	8.7	58
32	Boosting photo-Fenton process enabled by ligand-to-cluster charge transfer excitations in iron-based metal organic framework. Applied Catalysis B: Environmental, 2022, 302, 120882.	20.2	58
33	Cathode-Introduced Atomic H* for Fe(II)-Complex Regeneration to Effective Electro-Fenton Process at a Natural pH. Environmental Science & Technology, 2019, 53, 6927-6936.	10.0	54
34	Hydrodynamics of upflow anaerobic sludge blanket reactors. AICHE Journal, 2009, 55, 516-528.	3.6	52
35	Biochar enhanced biological nitrobenzene reduction with a mixed culture in anaerobic systems: Short-term and long-term assessments. Chemical Engineering Journal, 2018, 351, 912-921.	12.7	52
36	Two-stage chromium isotope fractionation during microbial Cr(VI) reduction. Water Research, 2019, 148, 10-18.	11.3	51

#	Article	IF	CITATIONS
37	High power generation in mixed-culture microbial fuel cells with corncob-derived three-dimensional N-doped bioanodes and the impact of N dopant states. Chemical Engineering Journal, 2020, 399, 125848.	12.7	51
38	Drag Coefficient of Porous and Permeable Microbial Granules. Environmental Science & Technology, 2008, 42, 1718-1723.	10.0	50
39	Simultaneous debromination and mineralization of bromophenol in an up-flow electricity-stimulated anaerobic system. Water Research, 2019, 157, 8-18.	11.3	50
40	Permeabilities of anaerobic CH4-producing granules. Water Research, 2006, 40, 1811-1815.	11.3	49
41	Bioelectrochemical system for recalcitrant p-nitrophenol removal. Journal of Hazardous Materials, 2012, 209-210, 516-519.	12.4	45
42	Fabrication of polypyrrole/β-MnO 2 modified graphite felt anode for enhancing recalcitrant phenol degradation in a bioelectrochemical system. Electrochimica Acta, 2017, 244, 119-128.	5.2	45
43	Comprehensive comparison of bacterial communities in a membrane-free bioelectrochemical system for removing different mononitrophenols from wastewater. Bioresource Technology, 2016, 216, 645-652.	9.6	44
44	Bioaugmentation potential of a newly isolated strain Sphingomonas sp. NJUST37 for the treatment of wastewater containing highly toxic and recalcitrant tricyclazole. Bioresource Technology, 2018, 264, 98-105.	9.6	44
45	Redox mediator-modified biocathode enables highly efficient microbial electro-synthesis of methane from carbon dioxide. Applied Energy, 2020, 274, 115292.	10.1	44
46	Dehalogenation of Iodinated X-ray Contrast Media in a Bioelectrochemical System. Environmental Science & Technology, 2011, 45, 782-788.	10.0	43
47	Role of molecular structure on bioelectrochemical reduction of mononitrophenols from wastewater. Water Research, 2013, 47, 5511-5519.	11.3	42
48	Metal Respiratory Pathway-Independent Cr Isotope Fractionation during Cr(VI) Reduction by <i>Shewanella oneidensis</i> MR-1. Environmental Science and Technology Letters, 2017, 4, 500-504.	8.7	42
49	Undiscovered Mechanism for Pyrogenic Carbonaceous Matter-Mediated Abiotic Transformation of Azo Dyes by Sulfide. Environmental Science & Technology, 2019, 53, 4397-4405.	10.0	42
50	Temperature dependence of bioelectrochemical CO2 conversion and methane production with a mixed-culture biocathode. Bioelectrochemistry, 2018, 119, 180-188.	4.6	40
51	Highly selective hydrogenation of CO 2 into formic acid on a nano-Ni catalyst at ambient temperature: Process, mechanisms and catalyst stability. Journal of CO2 Utilization, 2017, 19, 157-164.	6.8	36
52	Effects of Good's Buffers and pH on the Structural Transformation of Zero Valent Iron and the Oxidative Degradation of Contaminants. Environmental Science & Technology, 2018, 52, 1393-1403.	10.0	35
53	Structure-based synergistic mechanism for the degradation of typical antibiotics in electro-Fenton process using Pd–Fe3O4 model catalyst: Theoretical and experimental study. Journal of Catalysis, 2018, 365, 184-194.	6.2	35
54	Kinetics of reductive degradation of Orange II in aqueous solution by zero-valent iron. Journal of Chemical Technology and Biotechnology, 2004, 79, 1429-1431.	3.2	34

#	Article	IF	CITATIONS
55	Facilitated biological reduction of nitroaromatic compounds by reduced graphene oxide and the role of its surface characteristics. Scientific Reports, 2016, 6, 30082.	3.3	34
56	Differences in the colloid properties of sodium alginate and polysaccharides in extracellular polymeric substances with regard to membrane fouling. Journal of Colloid and Interface Science, 2019, 535, 318-324.	9.4	32
57	Enhanced hydrodeiodination of iodinated contrast medium by sulfide-modified nano-sized zero-valent iron: Kinetics, mechanisms and application prospects. Chemical Engineering Journal, 2020, 401, 126050.	12.7	31
58	Mixed-culture biocathodes for acetate production from CO2 reduction in the microbial electrosynthesis: Impact of temperature. Science of the Total Environment, 2021, 790, 148128.	8.0	31
59	Bioelectrochemical decolorization of a reactive diazo dye: Kinetics, optimization with a response surface methodology, and proposed degradation pathway. Bioelectrochemistry, 2019, 128, 9-16.	4.6	30
60	Role of NOM molecular size on iodo-trihalomethane formation during chlorination and chloramination. Water Research, 2016, 102, 533-541.	11.3	29
61	Nitrate stimulation of N-Methylpyrrolidone biodegradation by Paracoccus pantotrophus: Metabolite mechanism and Genomic characterization. Bioresource Technology, 2019, 294, 122185.	9.6	28
62	Removal of halogenated emerging contaminants from water by nitrogen-doped graphene decorated with palladium nanoparticles: Experimental investigation and theoretical analysis. Water Research, 2016, 98, 235-241.	11.3	26
63	Effect of surface modification on carbon nanotubes (CNTs) catalyzed nitrobenzene reduction by sulfide. Journal of Hazardous Materials, 2018, 357, 235-243.	12.4	26
64	Mechanistic study of Fe(III) chelate reduction in a neutral electro-Fenton process. Applied Catalysis B: Environmental, 2020, 278, 119347.	20.2	25
65	Electricity-stimulated anaerobic system (ESAS) for enhanced energy recovery and pollutant removal: A critical review. Chemical Engineering Journal, 2021, 411, 128548.	12.7	25
66	Optimization ofS/Fe ratio for enhanced nitrobenzene biological removal in anaerobicSystem amended withSulfide-modified nanoscale zerovalent iron. Chemosphere, 2020, 247, 125832.	8.2	23
67	Simultaneous removal of pyridine and denitrification in an integrated bioelectro-photocatalytic system utilizing N-doped graphene/α-Fe2O3 modified photoanode. Electrochimica Acta, 2021, 366, 137425.	5.2	22
68	Process and kinetics of azo dye decolourization in bioelectrochemical systems: effect of several key factors. Scientific Reports, 2016, 6, 27243.	3.3	20
69	Ag-TiO2/biofilm/nitrate interface enhanced visible light-assisted biodegradation of tetracycline: The key role of nitrate as the electron accepter. Water Research, 2022, 215, 118212.	11.3	20
70	Hydrodynamics of an Electrochemical Membrane Bioreactor. Scientific Reports, 2015, 5, 10387.	3.3	19
71	Aerobic removal of iodinated contrast medium by nano-sized zero-valent iron: A combination of oxidation and reduction. Journal of Hazardous Materials, 2019, 373, 417-424.	12.4	19
72	Catalytic CO ₂ reduction to valuable chemicals using NiFe-based nanoclusters: a first-principles theoretical evaluation. Physical Chemistry Chemical Physics, 2017, 19, 28344-28353.	2.8	18

#	Article	IF	CITATIONS
73	Simultaneous high-concentration pyridine removal and denitrification in an electricity assisted bio-photodegradation system. Chemical Engineering Journal, 2022, 430, 132598.	12.7	18
74	Potential regulates metabolism and extracellular respiration of electroactive <i>Geobacter</i> biofilm. Biotechnology and Bioengineering, 2019, 116, 961-971.	3.3	17
75	Active N dopant states of electrodes regulate extracellular electron transfer of Shewanella oneidensis MR-1 for bioelectricity generation: Experimental and theoretical investigations. Biosensors and Bioelectronics, 2020, 160, 112231.	10.1	15
76	An MFC-Based Online Monitoring and Alert System for Activated Sludge Process. Scientific Reports, 2014, 4, 6779.	3.3	14
77	A modified two-point titration method for the determination of volatile fatty acids in anaerobic systems. Chemosphere, 2018, 204, 251-256.	8.2	14
78	Formation of iodo-trihalomethanes (I-THMs) during disinfection with chlorine or chloramine: Impact of UV/H2O2 pre-oxidation. Science of the Total Environment, 2018, 640-641, 764-771.	8.0	14
79	Efficient bioanode from poultry feather wastes-derived N-doped activated carbon: Performance and mechanisms. Journal of Cleaner Production, 2020, 271, 122012.	9.3	14
80	Modification of regenerated cellulose ultrafiltration membranes with multi-walled carbon nanotubes for enhanced antifouling ability: Field test and mechanism study. Science of the Total Environment, 2021, 780, 146657.	8.0	14
81	Metal organic framework decorated with molybdenum disulfide for visible-light-driven reduction of hexavalent chromium: Performance and mechanism. Journal of Cleaner Production, 2021, 318, 128513.	9.3	14
82	Electrical stimulation enhancing anaerobic digestion under ammonia inhibition: A comprehensive investigation including proteomic analysis. Environmental Research, 2022, 211, 113006.	7.5	14
83	Response of anodic biofilm to hydrodynamic shear in two-chamber bioelectrochemical systems. Electrochimica Acta, 2017, 258, 1304-1310.	5.2	13
84	Tailoring the Electrochemical Protonation Behavior of CO ₂ by Tuning Surface Noncovalent Interactions. ACS Catalysis, 2021, 11, 14986-14994.	11.2	13
85	Dehalogenation of diatrizoate using nanoscale zero-valent iron: impacts of various parameters and assessment of aerobic biological post-treatment. RSC Advances, 2017, 7, 27214-27223.	3.6	12
86	Modeling of acetate-type fermentation of sugar-containing wastewater under acidic pH conditions. Bioresource Technology, 2018, 248, 148-155.	9.6	12
87	Polyaniline-decorated honeycomb-like structured macroporous carbon composite as an anode modifier for enhanced bioelectricity generation. Science of the Total Environment, 2019, 696, 133980.	8.0	12
88	lodo-trihalomethanes formation during chlorination and chloramination of iodide-containing waters in the presence of Cu2+. Science of the Total Environment, 2019, 671, 101-107.	8.0	12
89	Size-Dependent Response of the Reductive Reactivity of Zerovalent Iron toward the Coexistence of Natural Organic Matter. ACS ES&T Engineering, 2021, 1, 1587-1596.	7.6	12
90	Structural characteristics and microbial function of biofilm in membrane-aerated biofilm reactor for the biodegradation of volatile pyridine. Journal of Hazardous Materials, 2022, 437, 129370.	12.4	12

#	Article	IF	CITATIONS
91	Coexistence of humic acid enhances the reductive removal of diatrizoate <i>via</i> depassivating zero-valent iron under aerobic conditions. Journal of Materials Chemistry A, 2020, 8, 14634-14643.	10.3	11
92	Enhanced reductive reactivity of zero-valent iron (ZVI) for pollutant removal by natural organic matters (NOMs) under aerobic conditions: Correlation between NOM properties and ZVI activity. Science of the Total Environment, 2022, 802, 149812.	8.0	11
93	Advances in interfacial engineering for enhanced microbial extracellular electron transfer. Bioresource Technology, 2022, 345, 126562.	9.6	11
94	The maximum specific hydrogen-producing activity of anaerobic mixed cultures: definition and determination. Scientific Reports, 2014, 4, 5239.	3.3	10
95	Treatment of iodine-containing water by the UV/NH2Cl process: Dissolved organic matters transformation, iodinated trihalomethane formation and toxicity variation. Water Research, 2021, 200, 117256.	11.3	9
96	Anchoring α-, β-, or γ-MnO ₂ into Polypyrrole Wrapping for Modifying Graphite Felt Anodes: The Effect of MnO ₂ Type on Phenol Degradation. Chemistry Letters, 2017, 46, 1769-1772.	1.3	8
97	Insights into short- and long-term effects of loading nickel nanoparticles on anaerobic digestion with flocculent sludge. Environmental Science: Nano, 2019, 6, 2820-2831.	4.3	7
98	Efficiency of sequential UV/H2O2 and biofilm process for the treatment of secondary effluent. Environmental Science and Pollution Research, 2019, 26, 577-585.	5.3	7
99	Progressive stress response of the anaerobic granular sludge to nickel nanoparticles: experimental investigations and mathematic modelling. Environmental Science: Nano, 2019, 6, 1536-1548.	4.3	6
100	Beyond traditional water splitting for energy-efficient waste-to-hydrogen conversion with an inorganic–carbon hybrid nanosheet electrocatalyst. Journal of Materials Chemistry A, 2021, 9, 5364-5373.	10.3	5
101	Biogas. , 2019, , 110-127.		4
102	Carbon nanotubes mediated chemical and biological decolorization of azo dye: Understanding the structure-activity relationship. Environmental Research, 2022, 210, 112897.	7.5	4
103	Nutrient limitation regulates the properties of extracellular electron transfer and hydraulic shear resistance of electroactive biofilm. Environmental Research, 2022, 212, 113408.	7.5	4
104	Surface characteristics of acidogenic sludge in H2-producing process. Journal of Water and Environment Technology, 2007, 5, 1-12.	0.7	2
105	Nano-sized Zero-Valent Iron Coupled with Sulfidation and Ferrous Implantation Enhances the Reduction–Oxidation Removal of Iodinated Contrast Medium. ACS ES&T Water, 2021, 1, 2128-2138.	4.6	2
106	Nitrogen-doped pyrogenic carbonaceous matter facilitates azo dye decolorization by sulfide: The important role of graphitic nitrogen. Chinese Chemical Letters, 2023, 34, 107326.	9.0	2
107	Generation of iodinated trihalomethanes during chloramination in the presence of solid copper corrosion products. Water Research, 2022, 220, 118630.	11.3	2
108	Bioelectrodegradation of Hazardous Organic Contaminants from Industrial Wastewater. , 2019, , 93-119.		1

#	Article	IF	CITATIONS
109	A fixed-point titration method for the determination of ammonium in anaerobic systems. Analytical Methods, 2018, 10, 3552-3556.	2.7	0
110	Microbial Electro-respiration Enhanced Biodegradation and Bioremediation: Challenges and Future Perspectives 2019 293-300		0

Perspectives. , 2019, , 293-300.